Surface characterization of carbonated recycled concrete fines and its effect on the rheology, hydration and strength development of cement paste

Ouyang, Xiaowei; Wang, Liquan; Xu, Shida; Ma, Yuwei; Ye, Guang

Citation (APA)
Ouyang, X., Wang, L., Xu, S., Ma, Y., & Ye, G. (2020). Surface characterization of carbonated recycled concrete fines and its effect on the rheology, hydration and strength development of cement paste. *Cement and Concrete Composites*, *114*, 1-10. Article 103809. https://doi.org/10.1016/j.cemconcomp.2020.103809

Important note
To cite this publication, please use the final published version (if applicable).
Please check the document version above.

Surface Characterization of Carbonated Recycled Concrete Fines and Its Effect on the Rheology, Hydration and Strength Development of Cement Paste

Xiaowei Ouyang[1, *], Liquan Wang[1], Shida Xu[1], Yuwei Ma[1], Guang Ye[2]

[1] Guangzhou University—Tamkang University Joint Research Center for Engineering Structure Disaster Prevention and Control, Guangzhou University, Guangzhou 510006, China

[2] Department of Materials and Environment (Microlab), Faculty of Civil Engineering and Geosciences, Delft University of Technology, 2628CN Delft, The Netherlands

Abstract: Carbonation treatment can effectively improve the performance of recycled concrete aggregate and fines due to the reactions of CO_2 with CH and C-S-H gel of cement paste. To better understand the mechanisms involved in the performance improvement, the surface properties of carbonated recycled cement paste powder (CRP) and its effect on the rheology, hydration and strength development of cement paste was studied. The results showed that during the carbonation, the surface of CRP was covered by a layer of amorphous silica gel. The generated $CaCO_3$ was wrapt by the silica gel and seldom exposed. The silica layer led to the poor flowability of CRP-cement paste due to that the silica gel on the surface of CRP has a strong affinity for H_2O. During the very early hydration, the silica gel dissolved and then $CaCO_3$ was exposed. $CaCO_3$ is capable of chemically absorbing Ca^{2+}, which facilitated the nucleation of C-S-H nuclei and stabilized the C-S-H phase. As a result, the C-S-H grew densely, uniformly and perpendicularly on the surface of CRP. In addition, the

chemically absorbing Ca^{2+} enabled the chemical bond to be formed between $CaCO_3$ and C-S-H. Due to increased C-S-H resulted from reactions of silica gel with CH at the interface and the stronger bond formed between $CaCO_3$ and C-S-H, the interface between CRP and hydration products was much stronger than that between recycled cement paste powder (RP) and hydration products.

Keywords: Carbonation treatment; Recycled concrete fines; Recycled concrete aggregate; Rheology; Hydration; Strength development

1. Introduction

Reusing the demolished concrete not only reduces the pollution caused by concrete production and waste disposal but also preserves natural resources. In general, the demolished concrete is recycled to produce aggregate. However, compared with natural aggregate, the recycled aggregate has the characteristics of high porosity, strong water absorption, poor bonding ability and low strength [1-4]. These drawbacks limit the wide application of recycled concrete. Using carbonation treatment can effectively improve the performance of recycled concrete [5-12]. This is attributed to the fact that CO_2 reacts with CH and C-S-H gel of cement paste adhere to recycled aggerate to reduce water absorption and the porosity, and improve the strength [13-15]. The waste cement paste powder generated in the production of recycled aggerate also has a better performance after carbonation treatment when used in concrete to replace part of cement [16].

Hydration products (mainly C-S-H and CH) and unhydrated cement clinker (mainly C_3S and C_2S) in recycled cement paste can react with CO_2 to form $CaCO_3$, amorphous silica gel and amorphous alumina-silica gel [14, 17-21]. The calcite can fill the pores and increase the density of cement paste. The formed amorphous silica gel

2

will react with CH, thus accelerates the early age hydration of cement and increases the amount of hydration products [9, 22, 23]. Furthermore, the calcite can also react with the aluminate phase in cement paste resulting in a denser and higher strength cement paste [16]. However, the carbonation mechanisms of CH and C-S-H in the recycled cement paste are still not fully understood [14, 24]. The surface properties of the particles determine the interactions of particles with H_2O and ions in the solution of cement paste. These interactions play a crucial role in the C-S-H nucleation and growth on the particles [25, 26], the strength of the interface between the particles and C-S-H [27] and rheology of the blended cement paste [28]. The surface properties have a significant influence on flowability, hydration and strength development of the blended cement paste. However, the surface properties of carbonated cement paste remain obscure.

Therefore, to deeply understand the mechanisms behind the performance improvement caused by carbonation treatment for recycled cement paste powder, as well as recycled aggregate, the surface properties of recycled cement paste (RP) and carbonated recycled cement paste powder (CRP) were first characterized in this paper. X-ray diffraction (XRD), thermogravimetric analysis (TGA), ^{29}Si NMR analysis and zeta potential test will be utilized. Parallel to the surface properties characterization, the rheology of cement paste made of RP and CRP was compared. The morphology of the hydrates on the surface of RP and CRP at different hydration times was observed using a scanning electron microscope (SEM). Furthermore, the mechanical properties of the interface between RP or CRP and hydration products were analyzed. The effect of carbonation treatment on the performance of recycled cement paste powder as a cement replacement in terms of the rheology, hydration and strength development was discussed.

2. Materials and Methods

2.1 Materials and mixture

The chemical composition of the ordinary Portland cement P II 42.5 used in this study is listed in Table 1. The RP was obtained by grinding the crushed cement paste specimens after hydration for 120 days. The cement used for the preparation of RP was also the ordinary Portland cement P II 42.5. CRP was produced by placing the RP in a carbonation chamber at a temperature of $20 \pm 2 °C$, relative humidity of $70 \pm 5\%$, CO_2 concentration of $20 \pm 3\%$ and pressure of 0.1 MPa for 12 days. The particle size distributions of PC, RP and CRP were determined by Mastersizer 2000 (Malvern instruments Ltd. UK), as shown in Fig. 1. It can be seen that the particle size of CRP is larger than that of RP. It is due to that in the carbonation process the silica gel generated from the carbonation made some particles stick together to form a big particle, and the new phase formed at the surface of RP also enlarged the particle-size. The mixture compositions of pure cement paste and the cement paste blended with RP and CRP are given in Table 2. The mixtures prepared for the microscopic observation of the crack propagation are denoted as R1 and C1, respectively. The mixtures prepared for morphology analysis of the hydration products on the surfaces of RP and CRP are referred to R2 and C2, respectively. In order to make the RP or CRP particles more discoverable in the morphological investigation of hydration products on their surface, the content of RP or CRP is set as 40% instead of 30%.

Table 1. Chemical compositions of P II 42.5 ordinary Portland cement (wt%).

Table 2. Mixture compositions of blended cement paste.

Fig. 1. Cumulative distribution (a) and volume distribution (b) of particle size of cement, RP and CRP.

2.2 X-ray diffraction analysis (XRD)

XRD analysis was performed to study the phase composition of RP and CRP using a Bruker D max/RB diffractometer (Billerica, MA, USA) applying CuK$_\alpha$ radiation (λ =1.5418Å). The samples were scanned from $2\theta = 5^o$ to $2\theta = 80^o$ with a step size of 0.02^o.

2.3 Thermogravimetric analysis (TGA)

The thermogravimetric data of the RP and CRP were collected using Perkin Elmer TGA4000 with a heating rate of 10 ^{o}C /min from 30 ^{o}C to 800 ^{o}C. A N$_2$-gas flowing atmosphere at 1.5 bar was used in this measurement.

2.4 NMR measurement

NMR measurements were performed using a VNMRS spectrometer (Varian Inc., USA) operating at a field strength of 14.09 tesla (600 MHz) with a 54 mm bore. The ^{29}Si operating frequency was 119.17 MHz. Powder samples were packed into zirconium dioxide standard double bearing 7.5-mm rotors. The spinning frequency for all samples was 6000 Hz and was stabilized to ±3 Hz using an internal stabilization device. The samples were collected for 2048 scans, which consist of a single pulse of width 3.6 µs followed by a relaxation delay of 3 s. All ^{29}Si chemical shift data were externally referenced to the TMS resonance.

2.5 Zeta potential test

To characterize the surface chemical properties of RP and CRP, zeta potential measurement was performed to study the interactions between the particle's surface

and Ca^{2+} in a model solution. With these interactions, the chemical properties of the surface can be characterized [25]. The Malvern Zetasizer Nano (Malvern Instruments Ltd. UK) was used in this study.

Ca^{2+} is an important ion in the pore solution of cement paste. The interactions of Ca^{2+} with the particle's surface play a key role in the C-S-H nucleation and growth on the particles [25, 27, 29]. Therefore, $Ca(OH)_2$ was used to prepare the model solutions. In this experiment, 12 model solutions with different Ca^{2+} concentrations from 0.2 to 20 mmol/l were designed to evaluate the effect of Ca^{2+} on particle surface potential.

2.6 SEM analysis

Morphological investigation of hydration products at a very early age and crack characterization of cement paste at a late age was performed using Phenom ProX electron microscope (Phenom, FEI). Sample preparations for the morphological investigation are as follows:

1) The mixtures for investigating the hydrates on the surface of RP and CRP are shown in Table 2 (R2 and C2). At each required time (15min, 1, 4 and 7h), about 1g of the cement paste with RP or CRP was taken to stop hydration by using anhydrous alcohol. The samples in the alcohol were filtered and dried in a 35 ºC oven for 12 hours. The dried powder was then collected for the morphological investigation.

2) The mixtures for crack characterization are shown in Table 2 (R1 and C1). The samples were prepared according to the standard procedure of ASTM C305 [30]. At the ages of 7, 28, 96 and 120d, the samples were loaded under compression stress of 80% of the peak load for 5 seconds. After loading, the specimens were taken to stop hydration using anhydrous alcohol. Then, the samples were submerged in an epoxy resin. After epoxy resin hardened, the

samples were ground and polished for the morphological investigation of cracks propagation.

2.7 Rheological measurement

A rheometer (Brookfield DV3T model) with a coaxial cylinder geometry was used to test the rheological properties of the cement paste blended with RP and CRP. The mixtures for this test are shown in Table 2 (R1 and C1). An 80 seconds pre-shear at 100 s^{-1} followed by 60 seconds of rest was involved before the test. Afterward, the strain rate was increased gradually over 60 seconds to a final value of 100 s^{-1}. Bingham-Plastic model was applied to fit the shear stress versus strain-rate curves.

3. Results and discussion

3.1 Material characterization

3.1.1 XRD analysis

XRD data is shown in Fig. 2. As can be seen, RP and CRP have different XRD patterns. The crystalline phase of RP is mainly CH and ettringite (AFt). The diffraction peak of C_2S and C_3S also shows in RP indicating unhydrated cement remained in RP. The main crystalline phase in CRP is $CaCO_3$. This indicates that most of CH, AFt, C_2S and C_3S in RP had reacted with CO_2 to form $CaCO_3$ during carbonation.

Fig. 2. XRD patterns of RP and CRP.

3.1.2 TGA analysis

The thermal decomposition of RP and CRP obtained by TGA-DTG analyses is shown in Fig. 3. The TG/DTG spectra of RP shows a weight loss between 100 °C and

300 °C, corresponding to the dehydration of C-S-H and AFt. The steep weight loss between 400 °C and 500 °C refers to the dehydroxylation of CH. A small weight loss after 600 °C from the decarbonation of $CaCO_3$ indicates the presence of the natural carbonation in RP. Compared with RP, the TG/DTG spectra of CRP shows a steep weight loss after 550 °C and only a small amount of weight loss before 550 °C. These results are matched with the findings in XRD analysis. The calculation based on the TGA-DTG results indicates that about 12.46% CH and 8.30% $CaCO_3$ existed in RP, 4.03% CH and 52.30% $CaCO_3$ were present in CRP.

Fig. 3. Thermal decomposition of RP and CRP by TGA-DTG analyses.

3.1.3 ^{29}Si NMR analysis

The ^{29}Si MAS NMR spectra of RP and CRP is presented in Fig. 4. In silicate minerals, Q^n (n = 0, 1, 2, 3, 4) is commonly used to represent the chemical environment of ^{29}Si atoms, and n represents the number of shared oxygen atoms in each silicon-oxygen tetrahedron. The range of chemical shifts indicates different polymerization states of Si [18, 31-34]. Polymerization state of Si corresponds to different chemical displacement intervals. Five polymerization states of Si in silicon-oxygen tetrahedron can be characterized by ^{29}Si NMR test. The change from Q^0 to Q^4 indicates the increasing degree of polymerization of silicon-oxygen tetrahedron. Q^0 refers to an isolated silica tetrahedron commonly found in cement clinkers. Q^1 denotes a silicon-oxygen tetrahedron connected to only one $[SiO_4]$, which originates from the C-S-H phase. Q^2 refers to the silicon-oxygen tetrahedron connected with two silicon-oxygen tetrahedra, mainly from cement hydration to form C-S-H. Q^3 represents the silicon-oxygen tetrahedron linked to the other three silicon-oxygen tetrahedra, and Q^4 refers to

the structure of a three-dimensional network with four silicon-oxygen tetrahedra. Q^3 and Q^4 mainly exist in silica gel [35, 36].

As can be seen from Fig. 4, the ^{29}Si MAS NMR spectra of RP shows the characteristic peaks of RP with the resonance of Q^0 (-74.9 ppm), Q^1 (-82.9 ppm) and Q^2 (-87.8 ppm). It indicates that Si in RP mainly comes from unhydrated cement (Q^0) and C-S-H (Q^1 and Q^2). The main characteristic peaks of CRP shift to Q^3 (-90.5 ppm) and Q^4 (-104.5 ppm) corresponding to the silica gel. It is also noted that a small shoulder at Q^0 (-74.9 ppm) exists in CRP, which is attributed to the insufficient carbonatization of recycled cement paste powder. The ^{29}Si MAS NMR results are strongly matched with the TGA-DTG results, as well as XRD analysis. Fig. 4 reveals that the carbonation decreased the amount of unhydrous phases (Q^0) and C-S-H (Q^1 and Q^2), and increased the amount of silica gel (Q^3 and Q^4). It indicates that most of the C-S-H and anhydrous phases in RP had reacted with CO_2 to form silica gel.

Fig. 4. ^{29}Si NMR patterns of RP and CRP.

3.1.4 Morphology analysis

Morphology of RP and CRP was observed by SEM, as shown in Fig. 5. As can be seen, the surface of RP and CRP is not significantly different. The $CaCO_3$ resulted from the carbonation in CRP is not observed from the SEM figures. Another product of carbonation, silica gel, is also hard to be distinguished since it has no clear shape and structure as a non-crystallized and amorphous material. It is likely that the products covered the surface of the CRP particle are silica gel.

Fig. 5. Morphology of RP (a, b) and CRP (c, d).

3.1.5 Surface chemical properties analysis

Zeta potential test was performed to characterize the surface charge properties of RP and CRP, which are correlated with the surface chemical properties. The zeta potential of RP and CRP, together with the reference particles of limestone powder (LP), quartz powder and C-S-H particles tested by Helene et al. [37] in $Ca(OH)_2$ solutions is shown in Fig. 6. As can be seen, compared with quartz and CRP, RP has a higher potential at low Ca^{2+} concentration (<2 mmol/L) because of the dissolution of $Ca(OH)_2$ on its surface. When the concentration of Ca^{2+} exceeds 2 mmol/L, the RP and CRP have similar zeta potential as quartz powder and C-S-H. It indicates that the surface chemical properties of RP and CRP are similar to quartz and C-S-H, both of which are rich in silica phase. This is not consistent with the expectation that CRP is rich in calcium carbonate and that its surface potential should be similar to that of limestone particles with much higher zeta potential. The silica phase on the surface of CRP is thus believed to be a silica gel resulted from a carbonation reaction rather than $CaCO_3$. The generated $CaCO_3$ was likely wrapt within the silica gel layer instead of exposed.

Fig. 6. The zeta potential of RP and CRP as a function of Ca^{2+} concentration in $Ca(OH)_2$ solution.

3.2 Rheology of blended cement paste

Fig. 7 shows the shear stress versus a shear rate of pure cement paste and cement paste blended with 30% RP and CRP. It can be seen that the shear stress of CRP-cement paste is much higher compared with RP-cement paste through all tested shear rate. Considering that the surface charge properties of CRP and RP are similar, which play

10

an important role in the rheological properties of cement paste, the filler with higher surface area and smaller particle size should have a higher shear stress. The particle size of CRP (D_{50}: 55.41 µm) is significantly larger than that of CR (D_{50}: 22.23 µm), and the specific surface areas of CRP (0.56 m^2/g) is much less than that of CR (0.86 m^2/g). However, the shear stress of CRP-cement paste is significantly higher than that of RP-cement paste. It is possible due to RP has a favorable particle size distribution (PSD). The small particle in RP can fill up the voids and make they RP-cement paste more compact. Consequently, pore water can be released and the paste system would become more flowable.

However, the packing effect on the rheological properties is not that significant, as the smaller particle with a larger surface, on the other hand, needs more water to keep paste flow. It is believed that the silica gel on the surface of CRP plays a key role in the rheological properties of CRP-cement paste. As mentioned, the CRP's surface was covered with the silica gel. As is well known, the silica gel has a strong affinity for H_2O. As a result, a larger amount of water was absorbed on CRP's surface. It makes CRP-cement paste has much higher shear stress despite that it has a larger particle size and lower surface area.

The performance of carbonated cement paste powder seems contrary to the performance of carbonated recycled aggregate on the rheology. It was reported that the mortar or concrete with carbonated recycled aggregate has better flowability than that with uncarbonated recycled aggregate, due to carbonation reduces the porosity and thus water absorption of the recycled aggregate [11, 22, 38]. This can be explained by the fact that the recycled cement paste powder has a much larger surface area than the recycled aggregate. The surface area of recycled cement paste powder is around 1m^2/g, while the surface area of recycled aggregate is only about 0.001m^2/g. The effect of silica

gel of carbonated recycled aggregate on the water absorption is subtle. While the water absorption reduced because of the decrease of porosity in the carbonated recycled aggregate is significant. Therefore, carbonated recycled cement paste powder has a poor performance in flowability, whereas the carbonation of recycled aggregate enhances the performance in terms of flowability.

Fig. 7. Shear stress vs shear rate experimental data for cement paste and cement paste blended with 30% RP and 30% CRP.

3.3 Morphology of hydrates on the surface of RP and CRP

The morphology of the hydrates on the surface of RP and CRP particles at different hydration time is illustrated in Fig. 8. Fig. 8a and Fig. 8b (local enlarged image) show the surface of RP after hydration for 15 minutes. Fig. 8c and Fig. 8d (local enlarged image) present the surface of CRP after hydration for 15 minutes. At that time, there is no difference between the two particles and no hydration products are observed on their surface. After 1h hydration, as can be seen from Fig. 8e and Fig. 8f there are still no hydration products on the surface of RP. Whereas, there are many granular substances on the surface of CRP, which are probably C-S-H nuclei, as shown in Fig. 8g and Fig. 8h. After 4 hours of hydration, there are still no hydration products on the surface of RP, as shown in Fig. 8i and Fig. 8j, while the granular nuclei on the surface of CRP grow into acicular C-S-H, as shown in Fig. 8k and Fig. 8l. After hydration for 7h, a bit of hydration product appears on the surface of RP particles (Fig. 8m and Fig. 8n), while the C-S-H further growth on the surface of CRP. This C-S-H gel presents a fine needle-like appearance and is perpendicular to the particle surface, as shown in Fig. 8o and Fig. 8p. Moreover, as can be seen from Fig. 8o the CRP's surface is covered by the perpendicular needle C-S-H. In the resulted from [25], it is concluded that the strong

chemical interactions between $CaCO_3$ and C-S-H enable the C-S-H to grow perpendicularly and uniformly on its surface. Therefore, it is believed that there is a $CaCO_3$ layer underneath the silica gel layer covered on the surface of CRP. When the CRP and cement particles mixed with water, the silica gel layer dissolves and reacts in the solution. It makes $CaCO_3$ exposed and provides a nucleation site for C-S-H.

Fig. 8. Morphology of hydration products on the surface of RP particle at 15min (a, b), 1h (e, f), 4h (i, j) and 7h (m, n), and CRP particle at 15min (c, d), 1h (g, h), 4h (k, l) and 7h (o, p).

3.4 Crack characterization

The differences in crack propagation originate from the interface properties. According to the previous studies [39-41], the crack propagations in the cement paste are governed by weak interfaces and local stress distribution. The weak interface has a high probability to crack. To understand the effect of carbonation treatment of recycled hardened cement paste powder on the strength development of cement paste, the bond strength between RP or CRP and hydration products was evaluated by characterizing the crack propagation in the cement pastes subjected to compressive loading. Based on the microscopic observation by SEM, crack propagations in cement pastes at the curing ages of 7, 28, 96 and 120d are illustrated in Fig. 9, 10, 11 and 12, respectively. The red boxes in these figures are used to mark the crack propagated alongside the RP or CRP particles corresponding to the weak bonding; The yellow boxes are used to mark the crack passed through the RP or CRP particles.

Fig. 9a, 10a, 11a and 12a show the cracks in the cement paste with 30% RP at the curing age of 7, 28, 96 and 120d, respectively. As can been seen from these figures, the number of cracks tend to propagate along with the RP particles decreases as increasing

curing age but not obvious. Moreover, the cracks propagating around the RP particles can be seen regardless of curing age. It indicates that the strength of the interface between matrix and RP particle is weak and further hydration cannot enhance the interface even though the overall strength of the paste increased.

Whereas, even at the curing age of 7d, there are few cracks propagated along with the CRP particles (Fig. 9b). At the curing age of 28, 96 and 120d, it is hard to find crack propagated through the interface between matrix and CRP particles, as shown in Fig. 10b, 11b and 12b. The cracks in the cement paste have an increasing tendency to propagate through the CRP particle as increasing curing age. It illustrates that CRP has a much stronger interface with hydration products than RP.

Fig. 9. Crack propagation in cement paste incorporating 30% RP (a), and 30% CRP (b) at 7 days (The red boxes mark the crack propagated alongside the RP or CRP particles and the red arrows indicate the RP or CRP particles).

Fig. 10. Crack propagation in cement paste incorporating 30% RP (a), and 30% CRP (b) at 28 days (The red boxes mark the crack propagated alongside the RP or CRP particles and the red arrows indicate the RP or CRP particles).

Fig. 11. Crack propagation in cement paste incorporating 30% RP (a), and 30% CRP (b) at 96 days (The red boxes mark the crack propagated alongside the RP or CRP particles, the yellow boxes refer to the crack passed through the RP or CRP particles, and the red arrows indicate the RP or CRP particles).

Fig. 12. Crack propagation in cement paste incorporating 30% RP (a), and 30% CRP (b) at 120 days (The red boxes mark the crack propagated alongside the RP or CRP particles, the yellow boxes refer to the crack passed through the RP or CRP particles, and the red arrows indicate the RP or CRP particles).

3.5 Discussion

Fig. 13 shows an overview of the effect of the carbonation treatment on the performance of the recycled cement paste powder as a cement replacement in terms of the rheology, hydration and strength development:

(a) Materials characterization. The analysis of XRD, TGA and NMR showed that during the carbonation, most of the C-S-H, CH and anhydrous phases in RP had reacted with CO_2 to form $CaCO_3$ and silica gel. Besides, the zeta potential measurement indicated that the surface of CRP was covered by silica-rich materials. It is supposed to be the silica gel resulted from carbonation reactions of CO_2 with CH and C-S-H gel. Furthermore, based on the observation of the C-S-H nucleation and growth on CRP's surface, it showed that the CRP's surface was covered by the perpendicular needle C-S-H after hydration for 7h (Fig. 8o). It is indicated that underneath of the silica gel is $CaCO_3$ since the strong chemical interactions between $CaCO_3$ and C-S-H enable the C-S-H to grow perpendicularly and uniformly on its surface. It is concluded that in this investigation the carbonated recycled cement paste particle was covered by a large amount of silica gel, underneath of it is $CaCO_3$, as shown in Fig. 13a. This conclusion is the key to understand the effect of carbonation treatment on the performance of the recycled cement paste powder as a cement replacement. As mentioned, the surface chemical properties of the particles determine the interactions with H_2O and ions in the solution of cement paste. These interactions play a crucial role in the C-S-H nucleation

and growth on the particles [25], the strength of the interface between the particles and hydrates [27] and rheology of the blended cement paste [28].

(b) Effect on rheology. From the materials characterization, it is concluded that the surface of CRP was covered with a layer of amorphous silica gel. As is well known, the silica gel has a strong affinity for H_2O. As a result, once the CRP mixed with water, a larger amount of water was absorbed on the surface of CRP particles, as shown in Fig. 13b. It is adverse to the flowability of the blended cement paste. Therefore, CRP-cement paste has much higher shear stress than the RP-cement paste despite that CRP has a larger particle size and lower surface area.

(c) Effect on hydration. The morphology of the hydrates on the surface of RP and CRP particles (Fig. 8) indicates that during the early hydration of cement, the silica gel layer on the surface of CRP particles dissolved and made $CaCO_3$ exposed to provide a nucleation site for C-S-H. The surface of $CaCO_3$ possesses a very high affinity for Ca^{2+}. As demonstrated in the previous study [25], the driving force of adsorbing Ca^{2+} ions on the $CaCO_3$ surface is a strong acid-base interaction. This chemical interaction facilitates the nucleation of C-S-H nuclei and stabilizes the C-S-H phase. As a result, the C-S-H grew uniformly and perpendicularly on the surface, as shown in Fig. 13c. In the case of RP particles, their surface is covered by the C-S-H phase since the CH on the surface dissolved during the hydration. As shown in the previous study [25], the C-S-H has no affinity for Ca^{2+}. The driving force of adsorbing Ca^{2+} ions on the C-S-H surface is the relatively weak electrostatic interaction. Consequently, less Ca^{2+} ions are adsorbed onto the surfaces of RP. It made the C-S-H hard to nucleate and grow on the surface of RP, so few C-S-H nuclei can be observed in Fig. 8.

(d) Effect on strength development. In general, the surface chemical properties of particles have a strong correlation with the interface bonding strength. Chemically

adsorbed Ca^{2+} onto the $CaCO_3$ surface results in the formation of a very strong bond between $CaCO_3$ and C-S-H, while C-S-H particle is bonded to silica particle by relatively weak electrostatic forces [27]. The surface of the CRP turned into a calcite phase after hydration for several hours, while the surface of the RP was still silica phase (C-S-H). Therefore, the interface between CRP and hydrates was much stronger than that between RP and hydrates. The silica gel on the surface of CRP reacts with CH to form C-S-H, as inferred from Fig 8, leading to a denser interface between CRP and matrix, also improved the interface strength.

Fig. 13. Schematic diagram of the effect of carbonation treatment of recycled cement paste powder on the rheology, hydration and strength development.

4. Conclusions

In this paper, the surface properties of the carbonated recycled cement paste powder were elucidated. The effect of carbonation treatment on the performance of the recycled cement paste powder as a cement replacement in terms of the rheology, hydration and strength development was investigated. Based on the results obtained in this study, the conclusions can be drawn as follows:

1. During the carbonation, the CRP's surface is believed to be covered by a layer of amorphous silica gel. The generated $CaCO_3$ was wrapt by the silica gel and seldom exposed.

2. CRP-cement paste showed a higher flowability than the RP-cement paste despite that CRP has a larger particle size and lower surface area. It is due to that the silica gel on the surface of CRP has a strong affinity for H_2O.

3. During the very early hydration, the C-S-H grew uniformly and perpendicularly on the surface of CRP, but there were few hydration products on the surface of RP. This is because after silica gel on the surface dissolved $CaCO_3$ exposed which facilitated nucleation of C-S-H.

4. CRP has a much stronger interface with hydration products than RP, due to the stronger bond formed between $CaCO_3$ and C-S-H, and increased C-S-H resulted from the reactions of silica gel with CH at the interface.

Acknowledgments

Reference

[1] i.l.B. Topçu, N.F. Günçan, Using waste concrete as aggregate, Cement and Concrete Research 25(7) (1995) 1385-1390.

[2] C.S. Poon, Z.H. Shui, L. Lam, H. Fok, S.C. Kou, Influence of moisture states of natural and recycled aggregates on the slump and compressive strength of concrete, Cement and Concrete Research 34(1) (2004) 31-36.

[3] Z.H. Duan, C.S. Poon, Properties of recycled aggregate concrete made with recycled aggregates with different amounts of old adhered mortars, Materials & Design 58 (2014) 19-29.

[4] J. Xiao, J. Li, C. Zhang, Mechanical properties of recycled aggregate concrete under uniaxial loading, Cement and Concrete Research 35(6) (2005) 1187-1194.

[5] C. Shi, Y. Li, J. Zhang, W. Li, L. Chong, Z. Xie, Performance enhancement of recycled concrete aggregate–a review, Journal of Cleaner Production 112 (2016) 466-472.

[6] D. Xuan, B. Zhan, C.S. Poon, Assessment of mechanical properties of concrete incorporating carbonated recycled concrete aggregates, Cement Concrete Composites 65 (2016) 67-74.

[7] J. Zhang, C. Shi, Y. Li, X. Pan, C.-S. Poon, Z. Xie, Influence of carbonated recycled concrete aggregate on properties of cement mortar, Construction and Building Materials 98 (2015) 1-7.

[8] B. Zhan, C. Poon, C. Shi, CO2 curing for improving the properties of concrete blocks containing recycled aggregates, Cement and Concrete Composites 42 (2013) 1-8.

[9] L. Li, C.S. Poon, J. Xiao, D. Xuan, Effect of carbonated recycled coarse aggregate on the dynamic compressive behavior of recycled aggregate concrete, Construction and Building Materials 151 (2017) 52-62.

[10] B. Zhan, C.S. Poon, Q. Liu, S. Kou, C. Shi, Experimental study on CO2 curing for enhancement of recycled aggregate properties, Construction and Building Materials 67 (2014) 3-7.

[11] J. Zhang, C. Shi, Y. Li, X. Pan, C.-S. Poon, Z. Xie, Performance enhancement of recycled concrete aggregates through carbonation, Journal of Materials in Civil Engineering 27(11) (2015) 04015029.

[12] M. Zajac, J. Skocek, P. Durdzinski, F. Bullerjahn, J. Skibsted, M.B. Haha, Effect of carbonated cement paste on composite cement hydration and performance, Cement and Concrete Research 134 (2020) 106090.

[13] S. Kashef-Haghighi, Y. Shao, S. Ghoshal, Mathematical modeling of CO 2 uptake by concrete during accelerated carbonation curing, Cement and Concrete Research 67 (2015) 1-10.

[14] A. Morandeau, M. Thiery, P. Dangla, Investigation of the carbonation mechanism of CH and CSH in terms of kinetics, microstructure changes and moisture properties, Cement and Concrete Research 56 (2014) 153-170.

[15] B. Wu, G. Ye, Development of porosity of cement paste blended with supplementary cementitious materials after carbonation, Construction Building Materials 145 (2017) 52-61.

[16] B. Lu, C. Shi, J. Zhang, J. Wang, Effects of carbonated hardened cement paste powder on hydration and microstructure of Portland cement, Construction Building Materials 186 (2018) 699-708.

[17] Z. Šauman, Carbonization of porous concrete and its main binding components, Cement and Concrete Research 1(6) (1971) 645-662.

[18] T.F. Sevelsted, J. Skibsted, Carbonation of C–S–H and C–A–S–H samples studied by 13 C, 27 Al and 29 Si MAS NMR spectroscopy, Cement and Concrete Research 71 (2015) 56-65.

[19] M. Zajac, J. Skibsted, J. Skocek, P. Durdzinski, F. Bullerjahn, M.B. Haha, Phase assemblage and microstructure of cement paste subjected to enforced, wet carbonation, Cement Concrete Research 130 (2020) 105990.

[20] M. Thiery, G. Villain, P. Dangla, G. Platret, Investigation of the carbonation front shape on cementitious materials: effects of the chemical kinetics, Cement concrete research 37(7) (2007) 1047-1058.

[21] P.A. Slegers, P.G. Rouxhet, Carbonation of the hydration products of tricalcium silicate, Cement and Concrete Research 6(3) (1976) 381-388.

[22] L. Li, J. Xiao, D. Xuan, C.S. Poon, Effect of carbonation of modeled recycled coarse aggregate on the mechanical properties of modeled recycled aggregate concrete, Cement and Concrete Composites 89 (2018) 169-180.

[23] C. Liang, B. Pan, Z. Ma, Z. He, Z. Duan, Utilization of CO2 curing to enhance the properties of recycled aggregate and prepared concrete: A review, Cement and Concrete Composites 105 (2020) 103446.

[24] J. Visser, Influence of the carbon dioxide concentration on the resistance to carbonation of concrete, Construction and Building Materials 67 (2014) 8-13.

[25] X. Ouyang, D.A. Koleva, G. Ye, K. Van Breugel, Insights into the mechanisms of nucleation and growth of C–S–H on fillers, Materials and Structures 50(5) (2017) 213.

[26] D. Hou, Z. Li, T. Zhao, P. Zhang, Water transport in the nano-pore of the calcium silicate phase: reactivity, structure and dynamics, Physical Chemistry Chemical Physics Pccp 17(2) (2014) 1411-1423.

[27] X. Ouyang, D.A. Koleva, G. Ye, K. van Breugel, Understanding the adhesion mechanisms between CSH and fillers, Cement and Concrete Research 100 (2017) 275-283.

[28] D.P. Bentz, C.F. Ferraris, S.Z. Jones, D. Lootens, F. Zunino, Limestone and silica powder replacements for cement: Early-age performance, Cement and Concrete Composites 78 (2017) 43-56.

[29] K. Scrivener, A. Ouzia, P. Juilland, A.K. Mohamed, Advances in understanding cement hydration mechanisms, Cement and Concrete Research 124 (2019) 105823.

[30] A. Standard, C305, Standard practice for mechanical mixing of hydraulic cement pastes and mortars of plastic consistency, Annual book of ASTM standards, 2006.

[31] S. Masse, H. Zanni, J. Lecourtier, J.-C. Roussel, A. Rivereau, 29Si solid state NMR study of tricalcium silicate and cement hydration at high temperature, Cement and concrete research 23(5) (1993) 1169-1177.

[32] E. Pustovgar, R.P. Sangodkar, A.S. Andreev, M. Palacios, B.F. Chmelka, R.J. Flatt, J.B. d'Espinose de Lacaillerie, Understanding silicate hydration from quantitative analyses of hydrating tricalcium silicates, Nat Commun 7 (2016) 10952.

[33] D. Hou, T. Li, P. Wang, Molecular dynamics study on the structure and dynamics of NaCl solution transport in the nanometer channel of CASH gel, Acs Sustainable Chemistry & Engineering (2018) acssuschemeng.8b02126-.

[34] D. Hou, J. Zhang, W. Pan, Y. Zhang, Z. Zhang, Nanoscale mechanism of ions immobilized by the geopolymer: A molecular dynamics study, Journal of Nuclear Materials 528 (2020) 151841.

[35] G.W. Groves, A. Brough, I.G. Richardson, C.M. Dobson, Progressive changes in the structure of hardened C3S cement pastes due to carbonation, Journal of the American Ceramic Society 74(11) (1991) 2891-2896.

[36] Y. Ikeda, Y. Yasuike, M. Kumagai, Y.-Y. PARK, M. HARADA, H. TOMIYASU, Y. TAKASHIMA, 29Si MAS NMR study on structural change of silicate anions with carbonation of synthetic 11Å tobermorite, Journal of the Ceramic Society of Japan 100(1165) (1992) 1098-1102.

[37] H. Viallis-Terrisse, A. Nonat, J.-C. Petit, Zeta-potential study of calcium silicate hydrates interacting with alkaline cations, Journal of colloid and interface science 244(1) (2001) 58-65.

[38] B.J. Zhan, D.X. Xuan, C.S. Poon, Enhancement of recycled aggregate properties by accelerated CO2 curing coupled with limewater soaking process, Cement and Concrete Composites 89 (2018) 230-237.

[39] M. Luković, E. Schlangen, G. Ye, Combined experimental and numerical study of fracture behaviour of cement paste at the microlevel, Cement and Concrete Research 73(0) (2015) 123-135.

[40] J.M. van Mier, Multi-scale interaction potentials (F − r) for describing fracture of brittle disordered materials like cement and concrete, Int J Fract 143(1) (2007) 41-78.

[41] X. Ouyang, G. Ye, K. van Breugel, Experimental and numerical evaluation of mechanical properties of interface between filler and hydration products, Construction and Building Materials 135 (2017) 538-549.

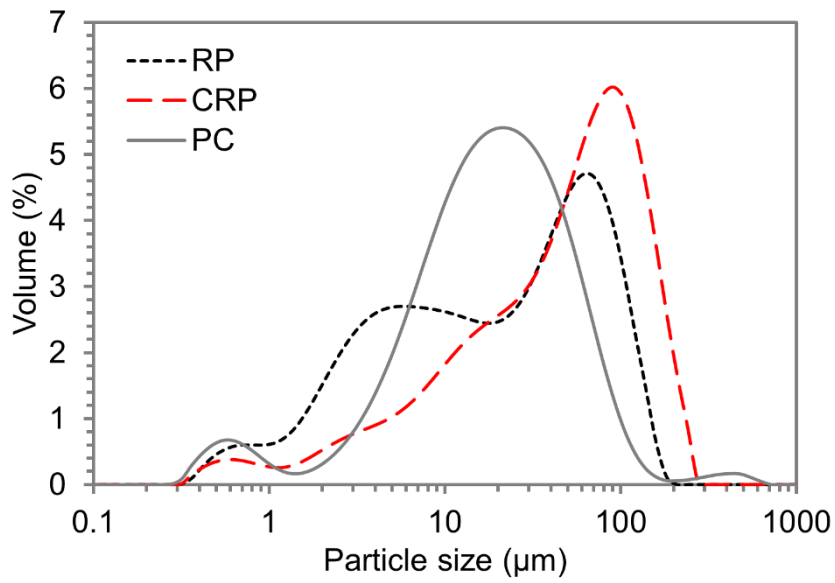**Table 1.** Chemical compositions of P II 42.5 ordinary Portland cement (wt%).

Components	SiO_2	Al_2O_3	Fe_2O_3	CaO	MgO	K_2O	SO_3	Loss
Cement	20.07	5.72	2.78	63.06	3.17	0.77	2.74	2.73

Table 2. Mixture compositions of blended cement paste.

Mixture	Cement (%)	RP (%)	CRP (%)	w/b
PC	100	-	-	0.4
R1	70	30	-	0.4
C1	70		30	0.4
R2	60	40		0.4
C2	60		40	0.4
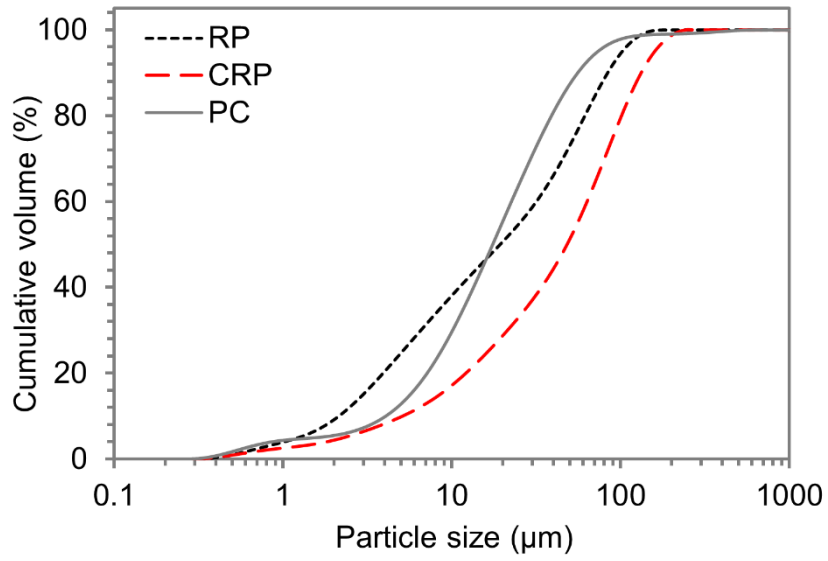
(a)

(b)

Figure 1. Cumulative distribution (a) and volume distribution (b) of particle size of cement, RP and CRP.
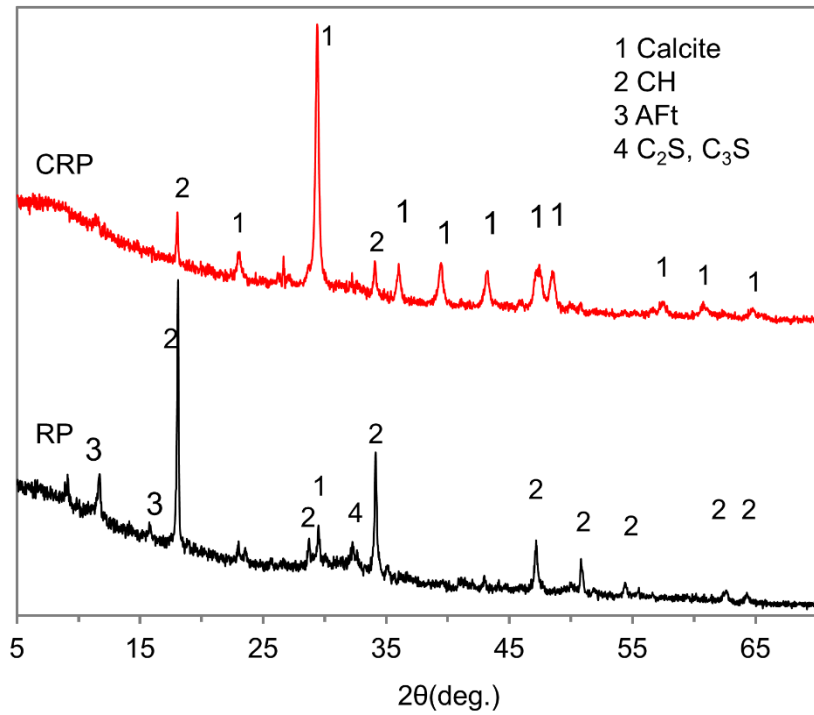
Figure 2. XRD patterns of RP and CRP.
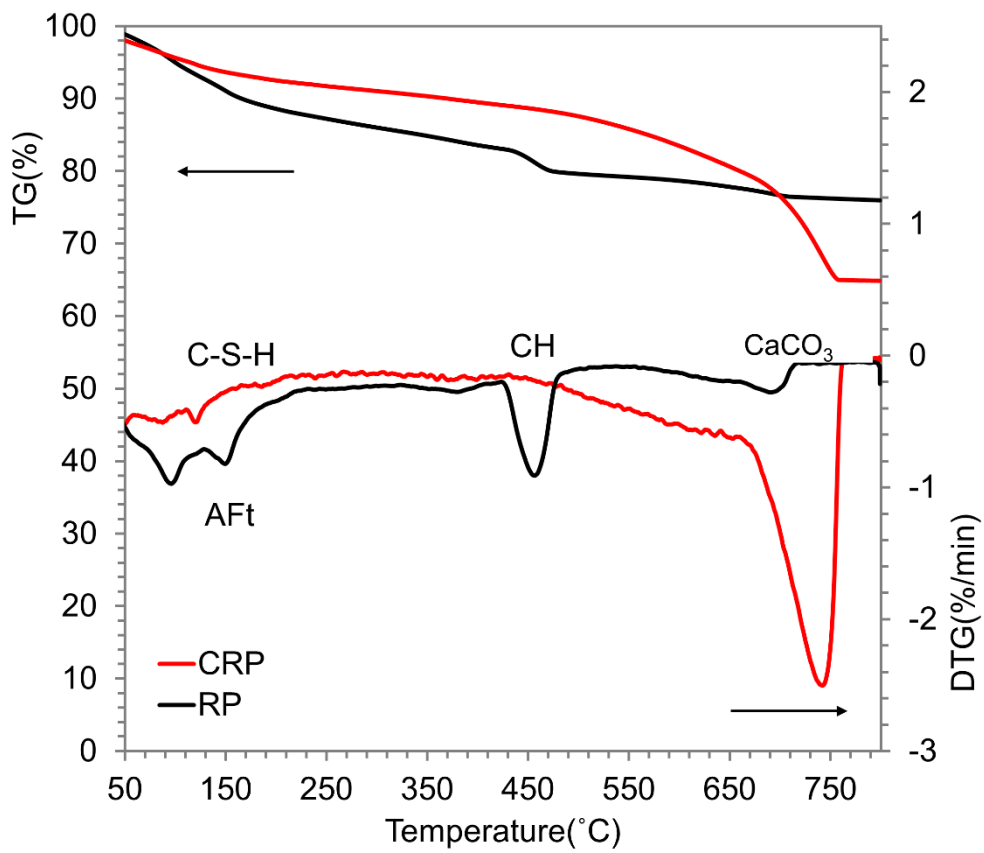
Fig. 3. Thermal decomposition of RP and CRP by TGA-DTG analyses.
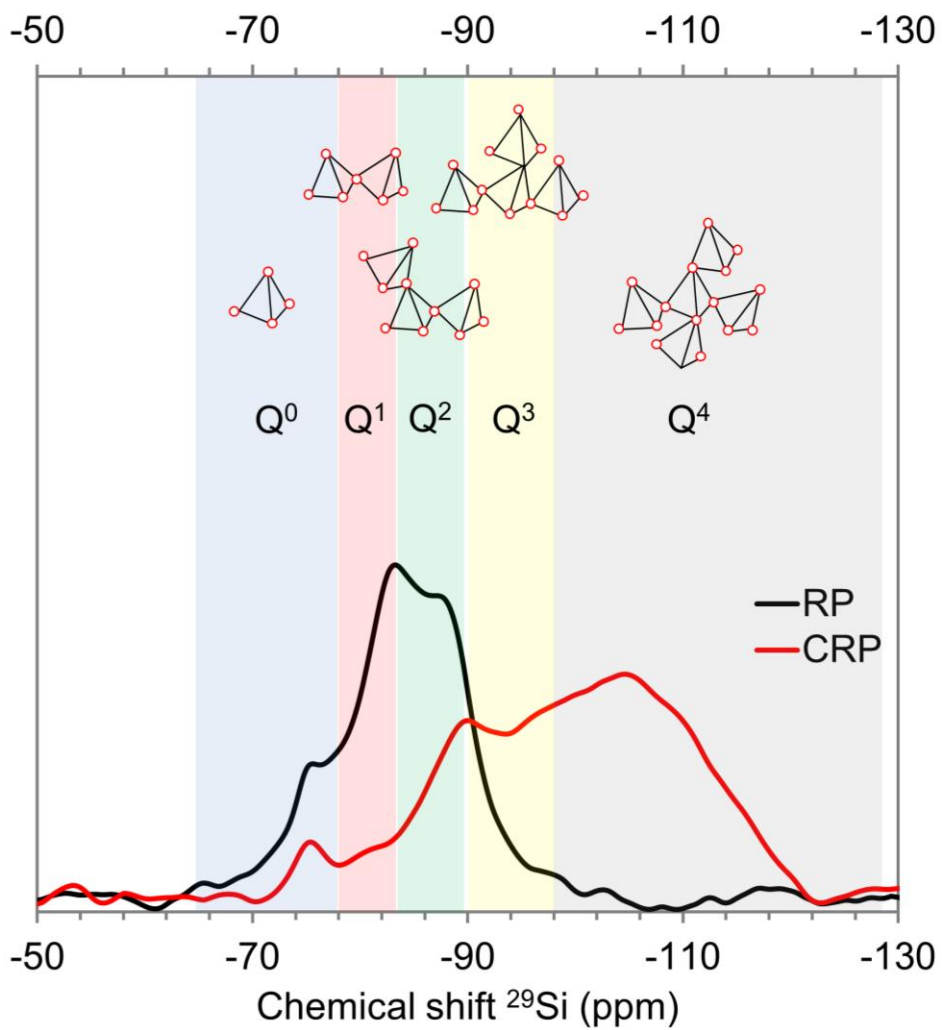
Fig. 4. ^{29}Si MAS NMR spectra for RP and CRP.
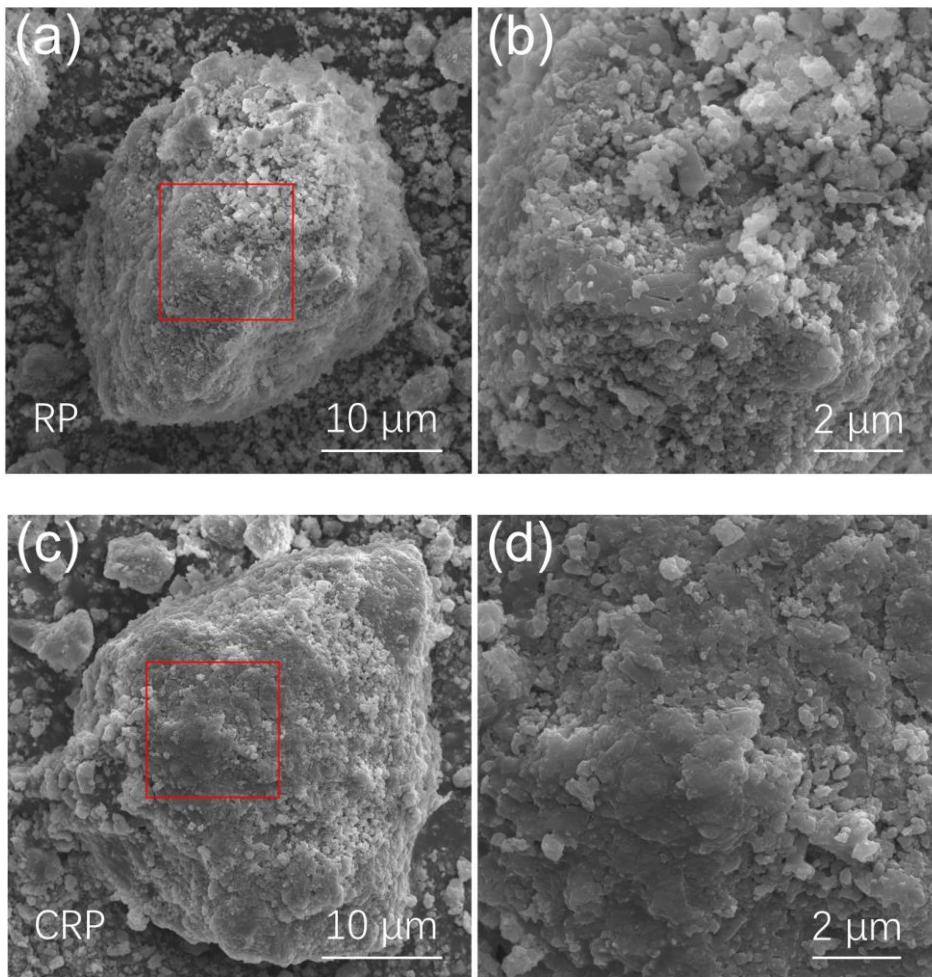
Fig. 5. Morphology of RP (a, b) and CRP (c, d).
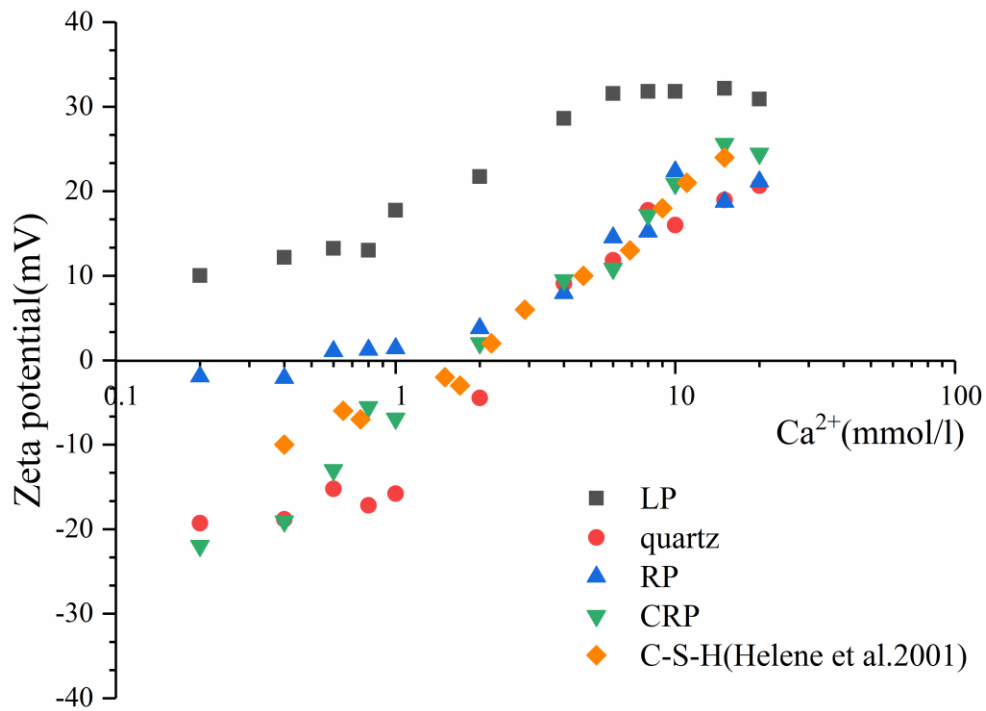
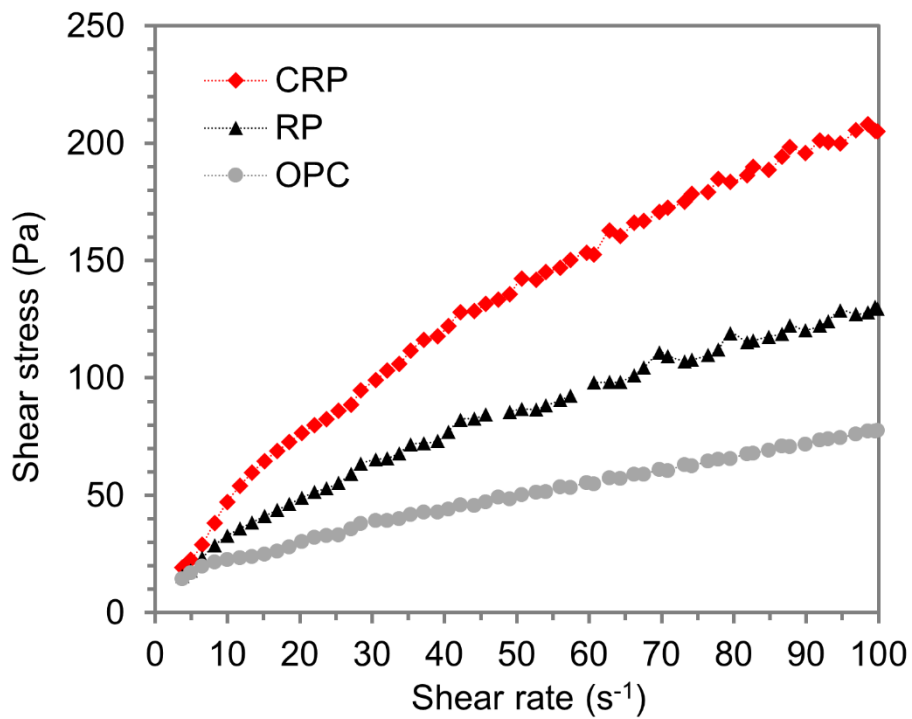**Fig. 6.** The zeta potential of RP and CRP as a function of Ca^{2+} concentration in Ca(OH)$_2$ solution.

Fig. 7. Shear stress vs shear rate experimental data for cement paste and cement paste blended with 30% RP and 30% CRP.
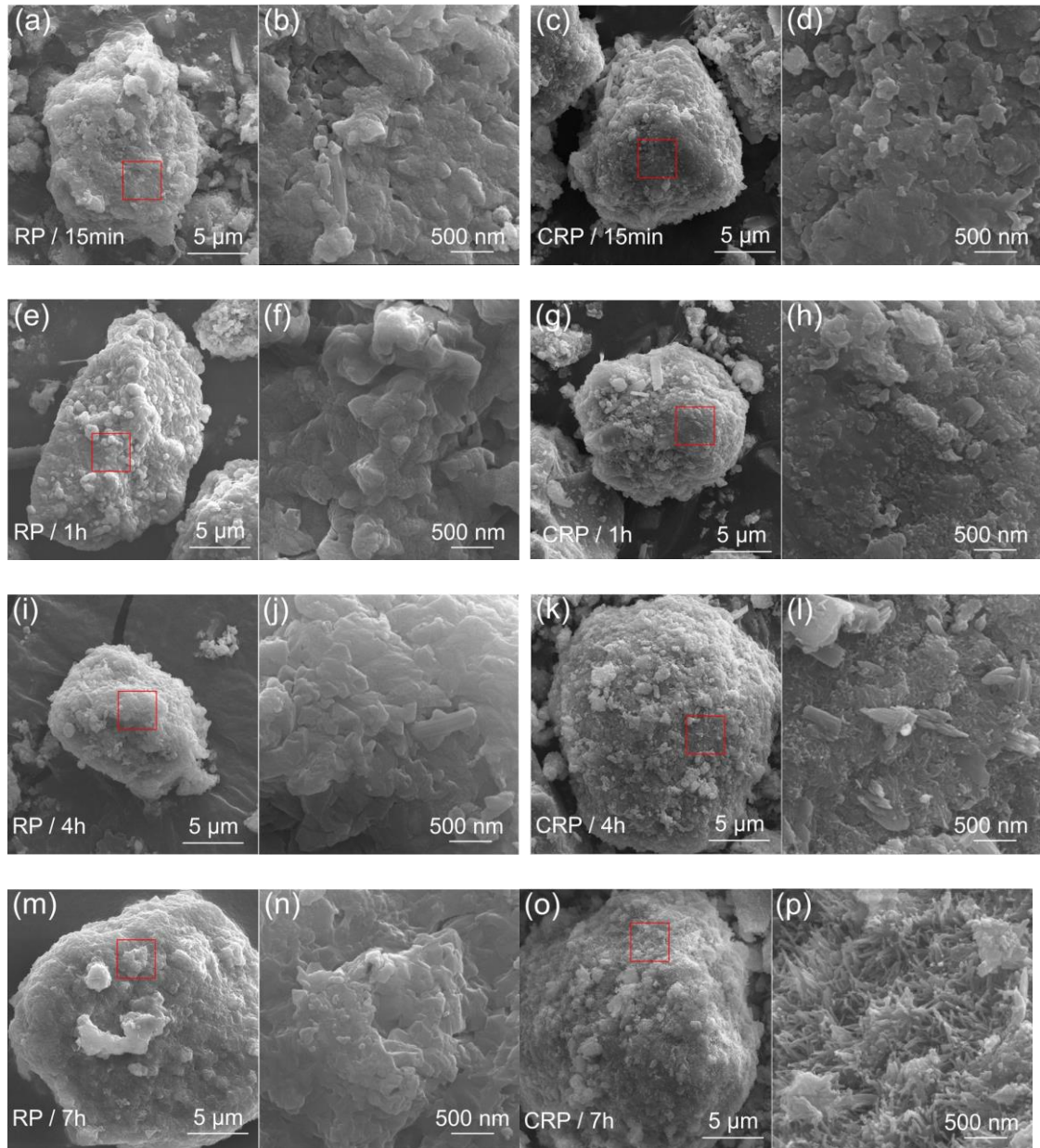
Fig. 8. Morphology of hydration products on the surface of RP particle at 15min (a, b), 1h (e, f), 4h (i, j) and 7h (m, n), and CRP particle at 15min (c, d), 1h (g, h), 4h (k, l) and 7h (o, p).

Fig. 9. Crack propagation in cement paste incorporating 30% RP (a), and 30% CRP

(b) at 7 days (The red boxes mark the crack propagated alongside the RP or CRP

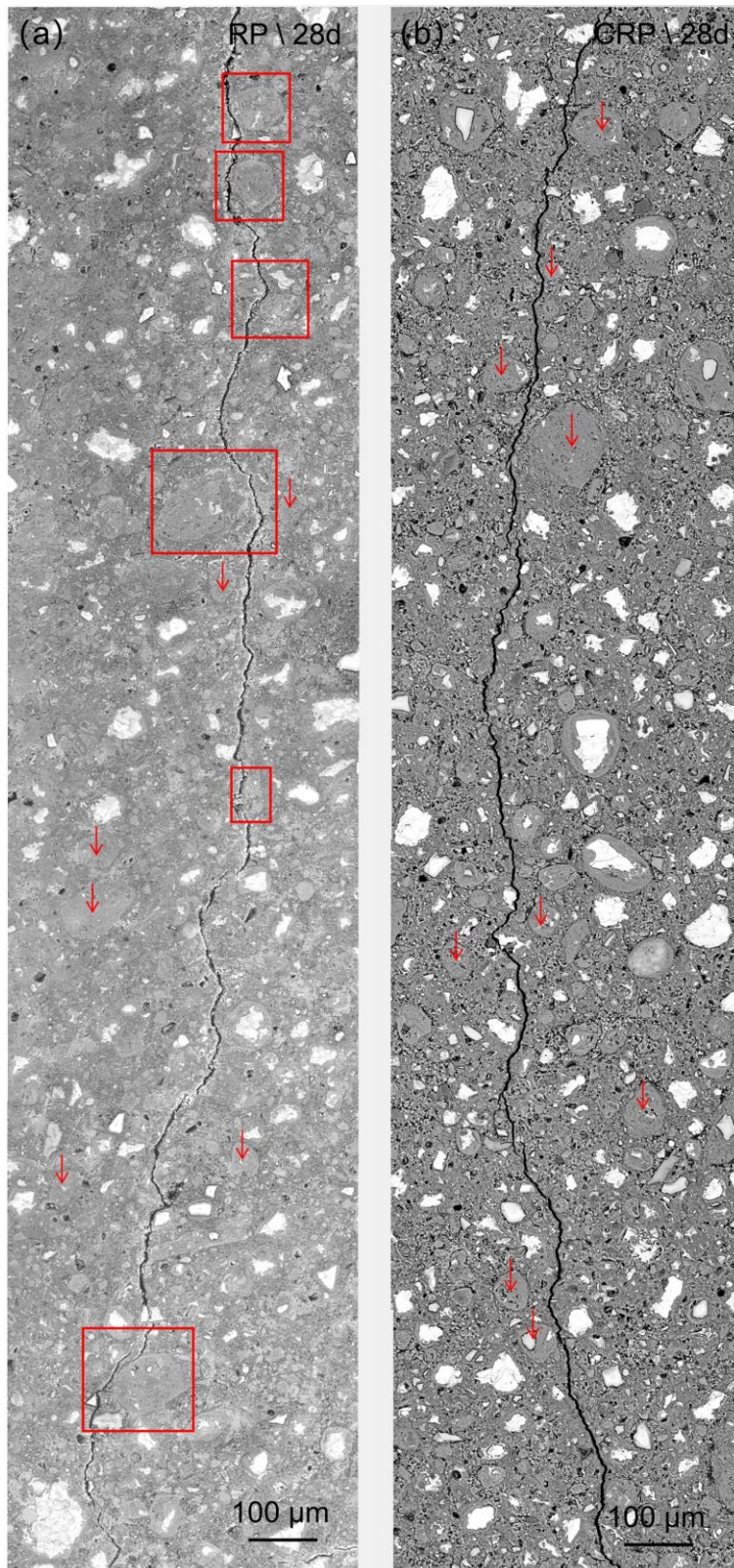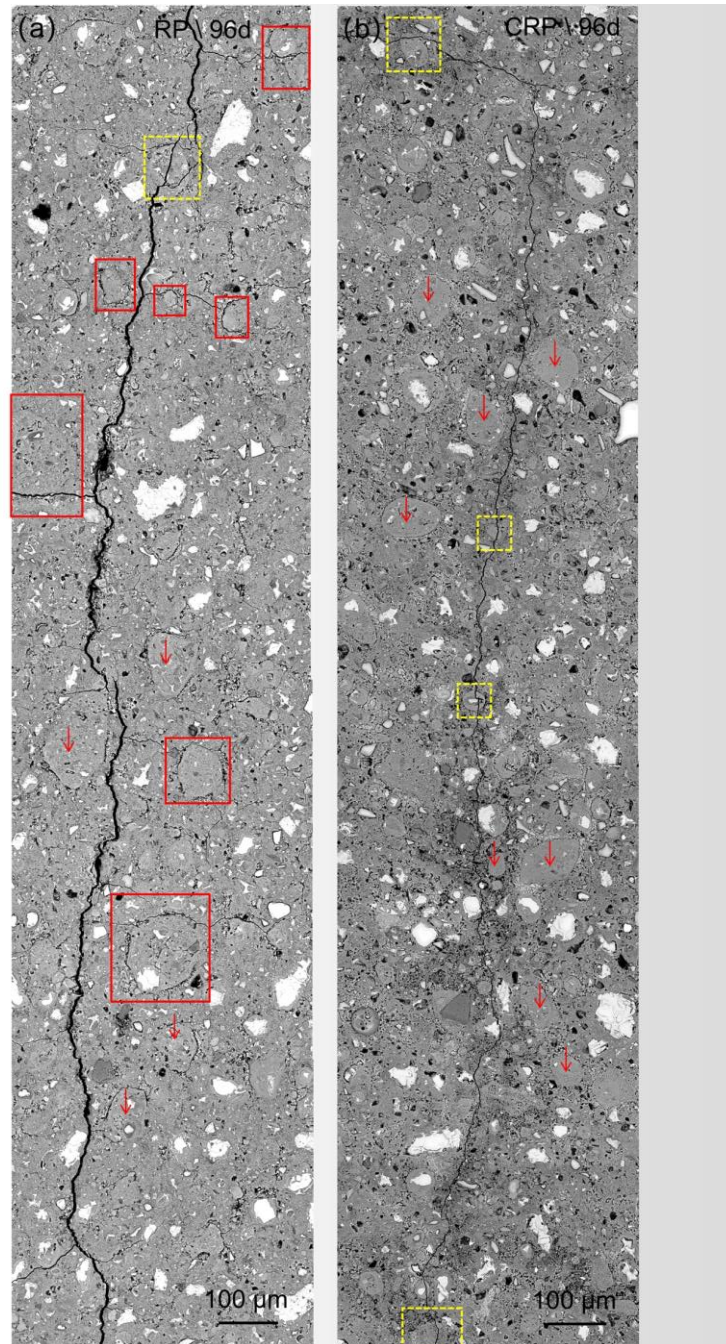particles and the red arrows indicate the RP or CRP particles).

Fig. 10. Crack propagation in cement paste incorporating 30% RP (a), and 30% CRP (b) at 28 days (The red boxes mark the crack propagated alongside the RP or CRP particles and the red arrows indicate the RP or CRP particles).

Fig. 11. Crack propagation in cement paste incorporating 30% RP (a), and 30% CRP (b) at 96 days (The red boxes mark the crack propagated alongside the RP or CRP particles, the yellow boxes refer to the crack passed through the RP or CRP particles, and the red arrows indicate the RP or CRP particles).
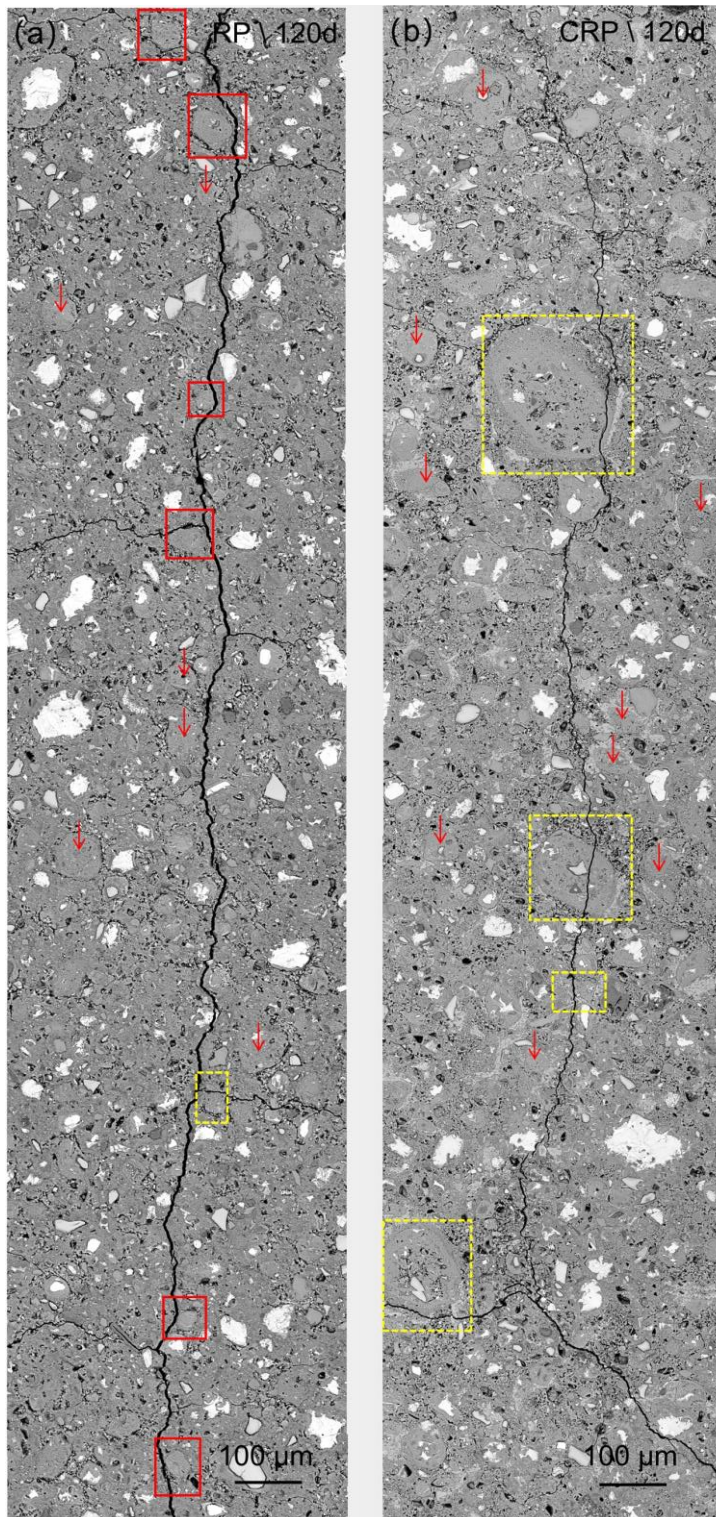
Fig. 12. Crack propagation in cement paste incorporating 30% RP (a), and 30% CRP (b) at 120 days (The red boxes mark the crack propagated alongside the RP or CRP particles, the yellow boxes refer to the crack passed through the RP or CRP particles, and the red arrows indicate the RP or CRP particles).
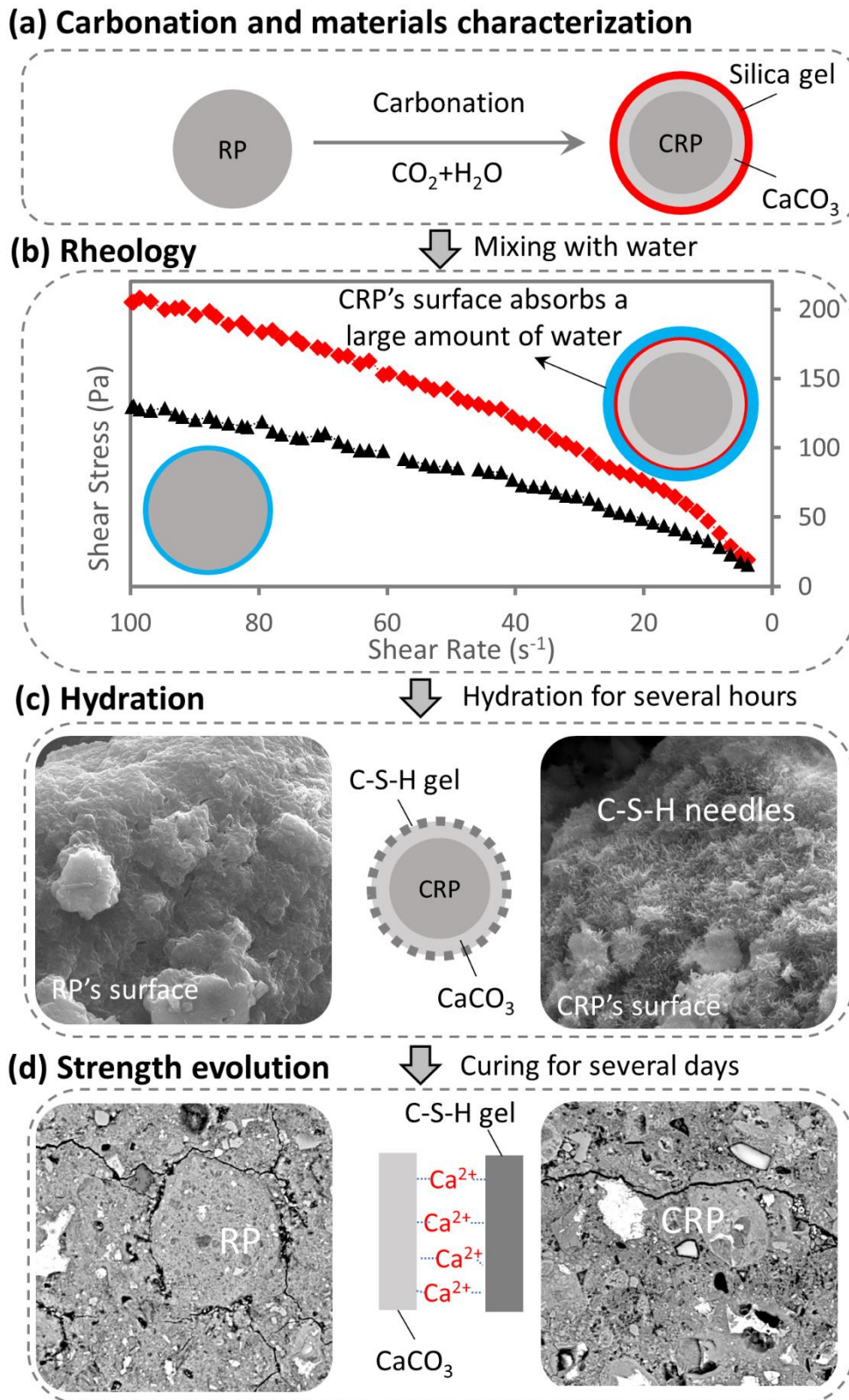
(a) Carbonation and materials characterization

(b) Rheology

(c) Hydration

(d) Strength evolution

Fig. 13. Schematic diagram of the effect of carbonation treatment of recycled cement paste powder on the rheology, hydration and strength development.